

Structure and microwave dielectric properties of $\text{Nd}_{(2-x)/3}\text{Li}_x\text{TiO}_3$

J.J. Bian*, G.X. Song, K. Yan

Department of Inorganic Materials, Shanghai University, 147 Yanchang Road, Shanghai 200072, China

Available online 29 September 2007

Abstract

The structure evolution, and microwave dielectric properties of $\text{Nd}_{(2-x)/3}\text{Li}_x\text{TiO}_3$ ceramics ($0 \leq x \leq 0.5$) were investigated in this paper. X-ray diffraction (XRD) and scanning electron microscopy (SEM) results show that samples with $x = 0.2$ – 0.4 exhibit single phase. Multi-phases of $\text{Nd}_2\text{Ti}_2\text{O}_7$, $\text{Nd}_{2/3}\text{TiO}_3$ and $\text{Nd}_2\text{Ti}_4\text{O}_{11}$ were observed when $x = 0$ and 0.1 . The concentration and ordering degree of A-site decrease with the increase of x value. The dielectric constant increases up to $x = 0.2$ and then decreases with the further increase of x value. The Qf value decreases with the increase of x value. The temperature coefficient of resonant frequency exhibits negative value and the absolute value decreases greatly with the decrease of x value.

© 2007 Elsevier Ltd and Techna Group S.r.l. All rights reserved.

Keywords: A-site deficient perovskite; Order–disorder; Microwave dielectric properties

1. Introduction

Complex perovskites with general formula $\text{A}^{2+}(\text{B}_{1/3}^{2+} \text{B}_{2/3}^{5+})\text{O}_3$ have received much attention in the wireless microwave communications community. Compared to the numerous examples of B-site ordered system, A-site ordered perovskites are relatively rare. A-site order–disorder reaction can play a critical role in affecting the properties of perovskites. Several studies have focused on the ionically conducting perovskites, $(\text{La}_{2/3-x}\text{Li}_{3x})\text{TiO}_3$ [1–3]. The ionic conductivities of the ordered A-site samples were approximately an order of magnitude lower than their disordered counterparts [1]. The A-site ordering degree of $(\text{La}_{(2-x)/3}\text{Li}_x)\text{TiO}_3$ was governed by the Li content and thermal treatment [3,4]. In Li poor compounds, the A-site cations adopt usual (0 0 1) ordered structure, while in Li-rich compounds ($x \geq 0.25$) or quenched samples, a disordered A-site structure was adopted. The crystal structures for different x values have not yet been well established until now and controversial results have been reported in the literature [5–7]. The phase diagram and crystal chemistry of the $\text{Li}_{0.5-3x}\text{RE}_{0.5+x}\text{TiO}_3$ (RE = La, Nd) systems have been studied by Robertson et al. [8]. Depending on the temperature and composition, three different polymorphs

labeled, α , β , and A, were found in the La system and four, α' , β , A, and C, in the Nd system [8]. The electron diffraction and high resolution electron microscopy study of the $\text{Li}_{0.5-3x}\text{Nd}_{0.5+x}\text{TiO}_3$ solid solution by Garcia-Martin et al. [9] shows that three (C, α' , and β) different polymorphs all adopt orthorhombic distorted perovskite structure most likely due to the tilting of the octahedra as it has been determined for the C-phase samples by neutron diffraction analysis [10]. A more complicated A-site ordering, which is not observed in the C-phase, existed in β -phase [8,9]. Recently authors have studied the structure and microwave dielectric properties of $\text{La}_{(2-x)/3}\text{Na}_x\text{TiO}_3$ [11]. The distribution (order–disorder) and concentration of vacancies, which may be interrelated, have considerable effect on the microwave dielectric properties of $\text{La}_{(2-x)/3}\text{Na}_x\text{TiO}_3$ [11]. The purpose of this paper is to systematically investigate the structure evolution and microwave dielectric properties of $\text{Nd}_{(2-x)/3}\text{Li}_x\text{TiO}_3$ ceramics ($0.0 \leq x \leq 0.5$).

2. Experimental procedure

$\text{Nd}_{(2-x)/3}\text{Li}_x\text{TiO}_3$ ($0.0 \leq x \leq 0.5$) ceramic samples were prepared by conventional solid-state reaction process from the starting materials including TiO_2 (99.9%), LiCO_3 (99.9%) and Nd_2O_3 (99.99%). The $\text{Nd}_{(2-x)/3}\text{Li}_x\text{TiO}_3$ ($0.0 \leq x \leq 0.5$) compounds were weighed and mixed with ZrO_2 balls in ethanol for 24 h, dried and calcined at the temperature of 1100 °C for 2 h in

* Corresponding author.

E-mail address: jjbian@shu.edu.cn (J.J. Bian).

a alumina crucible. The calcined powders were grounded, dried and mixed with 7 wt% PVA. The mixtures were pressed into pellets. The compacts were sintered ranging from 1250 to 1350 °C for 2 h. In order to prevent the Li-loss from evaporation, all samples were muffled with powders of the same composition during sintering.

The phase constitutes of the sintered samples were identified by X-ray powder diffraction (XRD) with Ni-filtered Cu K α radiation (Model Dmax-RC, Japan). Bulk density of the sintered specimens was identified by Archimedes' method. The Raman experiments were carried out for the sintered samples (Model Jobin Yvon U1000). A laser line of 532 nm and 500 mW average power was used. The spectra were recorded from 0 to 1000 cm⁻¹. The microstructure of the sintered sample was characterized by scanning electron microscopy (SEM) (Model XL20, Philips Instruments, Netherlands). All samples were polished and thermal etched at the temperature which was 70–100 °C lower than its sintering temperature. Microwave dielectric properties of the sintered samples were measured between 7 and 8 GHz using network analyzer (Hewlett Packard, Model HP8720C, USA). The quality factor was measured by the transmission cavity method. The relative dielectric constant (ϵ_r) was measured according to the Hakki–Coleman method using the TE₀₁₁ resonant mode, and the temperature coefficient of the resonator frequency (τ_f) was measured using invar cavity in the temperature range from –20 to 80 °C.

3. Results and discussion

Fig. 1 shows the XRD patterns of sintered Nd_{(2-x)/3}Li_xTiO₃ (0.0 ≤ x ≤ 0.5) samples, in which the Bragg reflections have been indexed according to Ref. [8]. Samples from x = 0.2 to 0.4 exhibit single β phase. The x = 0.5 sample contains additional trace amount of Nd₂Ti₂O₇ impurity phase, which is in agreement with the result reported by Robertson et al that Li_{0.5}Nd_{0.5}TiO₃ does not exist at any temperature under ambient conditions [8]. Small amount of Nd₂Ti₂O₇ and Nd₂Ti₄O₁₁ impurity phases appear for the sample with x = 0.1. For the sample with x = 0, the amount of Nd₂Ti₂O₇ and Nd₂Ti₄O₁₁ impurity phases increase greatly in addition to trace amount of

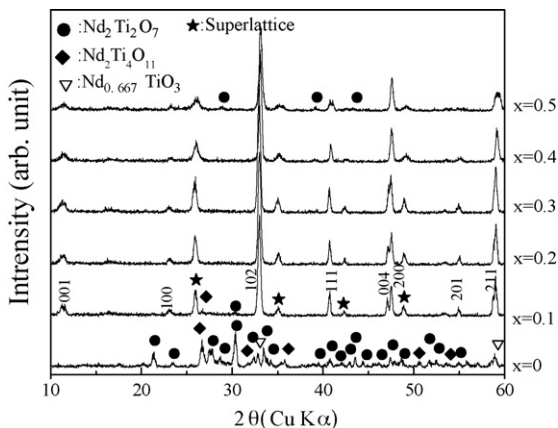


Fig. 1. XRD patterns of Nd_{(2-x)/3}Li_xTiO₃ (0 ≤ x ≤ 0.5) sintered at 1350 °C/2 h.

Nd_{2/3}TiO₃ phase. The superstructure reflections produced by A-site ordering (marked with asterisk) become decreased with the addition of Li⁺. It indicates that the A-site cation ordering degree decrease with the increase of lithium content. However, it still exists for the sample with x = 0.5, which is not like the case in La_{0.5}Na_{0.5}TiO₃. The reason may be related to the larger ionic difference on A-site for Nd_{(2-x)/3}Li_xTiO₃ than that of La_{(2-x)/3}Na_xTiO₃ ($\Delta R_{Li-Nd} = 0.51$ Å and $\Delta R_{La-Na} = 0.03$ Å) [12]. It is noted that the profiles of the fundamental (2 0 0) peak is splitted when x ≤ 0.3, which indicates the lower symmetry of the structure, while no splitting occurs when x > 0.3. It seems to imply some relevance between the peak splitting and the A-site ordering state. The splitting of (2 0 0) peak is caused by the distortion of TiO₆ octahedron which is resulted from the A-site ordering [4,5,11].

A room temperature Raman spectra of the samples with different lithium content are shown in Fig. 2. The Raman spectrum of Nd_{(2-x)/3}Li_xTiO₃ (0.1 ≤ x ≤ 0.5) in Fig. 2 shows five bands, which is in good agreement with that of La_{(2-x)/3}Na_xTiO₃ [11] except for the up shift of the bands due to the lighter Li atom compared to Na. According to the tetragonal approach of La_{(2-x)/3}Na_xTiO₃ the 141, 255 and 537 cm⁻¹ band can be assigned to be E_g symmetry species, while the 335 cm⁻¹ band behave like A_{1g} modes [3,11]. Some qualitatively trend can be observed that all bands are broadened and the intensities are decreased with the increase of lithium content. This may be related to the alleviation of TiO₆ distortion resulted from the decrease of A-site ordering, which is in good agreement with the XRD results. Another weak band near 471 cm⁻¹, which exists in all samples, may be due to the tilting of TiO₆. The cooperative tilting and rotating of octahedra is likely due to the combined effect of the smaller size of Nd cations compared with La³⁺ the Li ions in off-center sites, and the occurrence of A-site vacancies [9]. Based on the assumption that the perovskite-type structural framework is dominated by the larger rare earth ions other than small alkali ions, tolerance factor for Nd_{0.5}Li_{0.5}TiO₃ is calculated as 0.94. Both in-phase and anti-phase tilt should occur simultaneously for t < 0.965 [13]. The tilting of oxygen octahedra in perovskites should

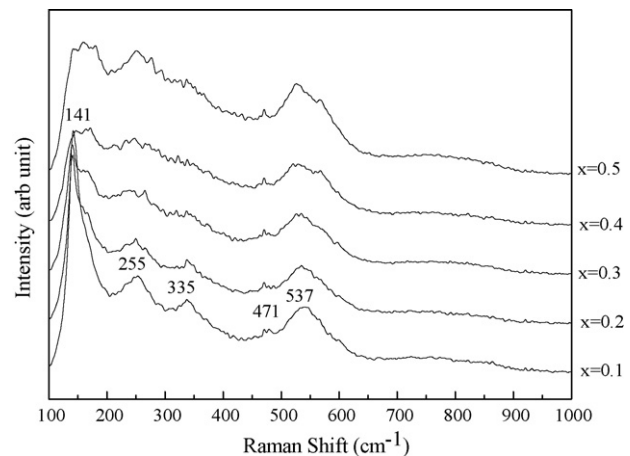


Fig. 2. Raman spectrum of the sintered Nd_{(2-x)/3}Li_xTiO₃ ceramics with different x values.

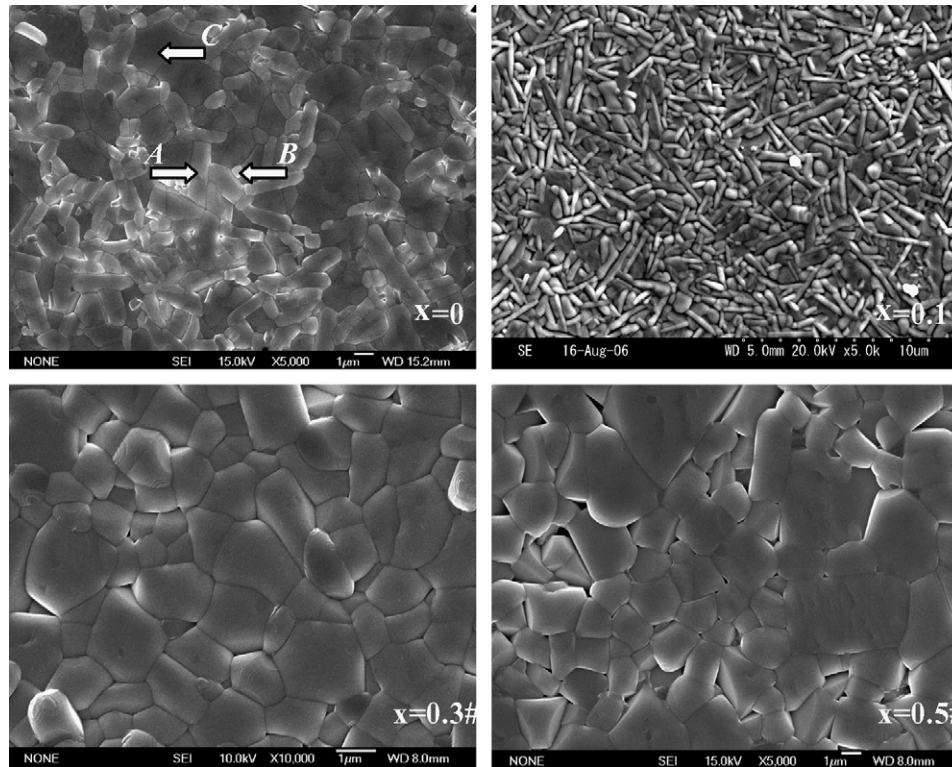


Fig. 3. SEM photographs of $\text{Nd}_{(2-x)/3}\text{Li}_x\text{TiO}_3$ ceramic sintered at $1300\text{ }^\circ\text{C}/2\text{ h}$ for $x = 0.0, 0.1, 0.3$ and 0.5 , respectively. (A: $\text{Nd}_2\text{Ti}_2\text{O}_7$, B: $\text{Nd}_2\text{Ti}_4\text{O}_{11}$ and C: $\text{Nd}_2/3\text{TiO}_3$).

cause superstructure reflections which is difficult to detect by XRD due to the weakness of reflections associated with small displacement of the oxygen atoms, while can be apparently detected by Raman scattering.

Fig. 3 shows the SEM photographs for the samples sintered at $1300\text{ }^\circ\text{C}/2\text{ h}$ for $x = 0.0, 0.1, 0.3$ and 0.5 , respectively. All sintered samples exhibit dense microstructures. EDS analysis of the sample with $x = 0$ exhibits mixture phase $\text{Nd}_{2/3}\text{TiO}_3$, $\text{Nd}_2\text{Ti}_2\text{O}_7$ and $\text{Nd}_2\text{Ti}_4\text{O}_{11}$, which is in agreement with the XRD results. From the SEM photos for the sample with $x = 0.1$, the amount of impurity phases seems larger than that of estimated from XRD analysis. It is related to the further evaporation of lithium during the thermal etching process.

Fig. 4 shows the variation of dielectric constants measured at microwave frequency as a function of x value for $\text{Nd}_{(2-x)/3}\text{Li}_x\text{TiO}_3$ sintered at different temperatures. The dielectric constant decreases slightly with the increase of x value when $x > 0.1$. According to the equation of Clausius–Mossotti (C–M), the dielectric constant increases with increasing total dielectric polarizability α_D and decreasing unit-cell volume. The unit-cell volume was estimated from the XRD data and changed a little from 55.97 \AA^3 for $x = 0.5$ sample to 56.35 \AA^3 for $x = 0.1$ sample. The effect of α_D on dielectric constant is much larger than that of unit-cell volume. A small change of α_D will result in large variation of dielectric constant [14]. The α_D in one primitive cell decreases with increasing Li content due to the fact that the ionic polarizability of Li^+ is much lower than that of Nd^{3+} ($\alpha_{\text{Nd}^{3+}}: 6.07\text{ \AA}^3$ and $\alpha_{\text{Li}^+}: 1.2\text{ \AA}^3$) [14]. So the dielectric constant should be decreased with increasing lithium content, which is in agreement with the results in Fig. 4. The

dielectric constant of the sample with $x = 0$ is 38, which is much lower than that of other compositions. It is obviously related to the existence of large amount of $\text{Nd}_2\text{Ti}_2\text{O}_7$ phase whose dielectric constant at microwave frequency was reported to be 36 [15]. The slight decrease of dielectric constant for the sample with $x = 0.1$ is also due to the existence of trace amount of low k $\text{Nd}_2\text{Ti}_2\text{O}_7$ phase.

The variation of Qf values as a function of lithium content is shown in Fig. 5. The Qf decreases as the lithium content increases, which is mainly due to the decrease of A-site ordering as discussed above. Fig. 6 shows the change of temperature coefficient of resonant frequency τ_f as a function of

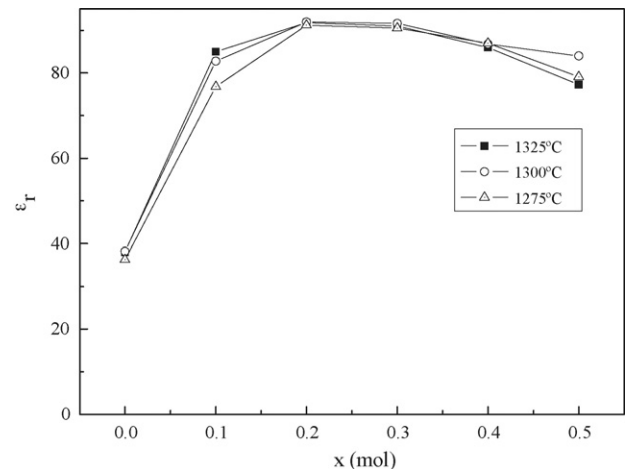


Fig. 4. Variation of dielectric constants as a function of x value for $\text{Nd}_{(2-x)/3}\text{Li}_x\text{TiO}_3$.

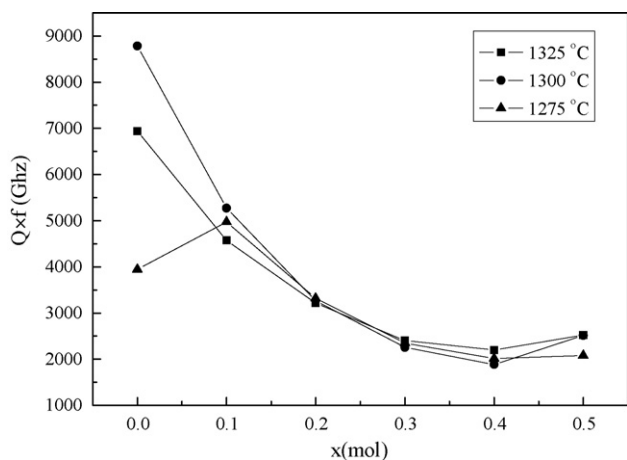


Fig. 5. Variation of Q_f value as a function of x value for $\text{Nd}_{2-x/3}\text{Li}_x\text{TiO}_3$.

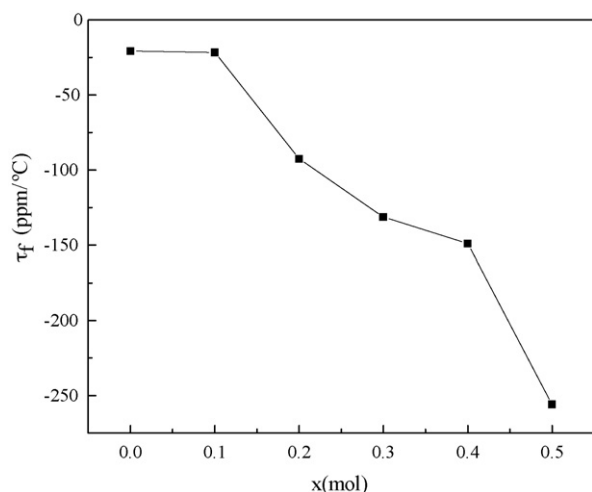


Fig. 6. Variation of τ_f value as a function of x value for $\text{Nd}_{2-x/3}\text{Li}_x\text{TiO}_3$.

lithium content. All samples exhibit negative τ_f value, and its absolute value decreases from 256 to about 20 ppm/°C as the lithium content decreases from $x = 0.5$ to 0.1. This may be related to the variation of tilting of TiO_6 -octahedra with the lithium content [13]. With the further decrease of x value until to $x = 0$, no further decrease of τ_f is observed. As discussed above, the sample with $x = 0$ exhibits mixture phases of $\text{Nd}_2\text{Ti}_2\text{O}_7$, $\text{Nd}_{2/3}\text{TiO}_3$ and $\text{Nd}_2\text{Ti}_4\text{O}_{11}$. The τ_f value of $\text{Nd}_2\text{Ti}_2\text{O}_7$ was reported to be -118 ppm/°C [12]. However we could not obtain the τ_f value of $\text{Nd}_{2/3}\text{TiO}_3$ due to the thermal instability of pure $\text{Nd}_{2/3}\text{TiO}_3$ in ambient atmosphere. We could not discuss its τ_f value by mixing law here.

4. Conclusions

The microstructure and microwave dielectric properties of $\text{Nd}_{2-x/3}\text{Li}_x\text{TiO}_3$ ceramics ($0.0 \leq x \leq 0.5$) have been studied in this paper. In conclusion, samples with $x = 0.2$ – 0.4 exhibit single phase. Multi-phases of $\text{Nd}_2\text{Ti}_2\text{O}_7$, $\text{Nd}_{2/3}\text{TiO}_3$ and $\text{Nd}_2\text{Ti}_4\text{O}_{11}$ were observed when $x = 0$ and 0.1. Additional

trace amount of $\text{Nd}_2\text{Ti}_2\text{O}_7$ was observed in $x = 0.5$ sample. The A-site ordering degree decreases with the increase of lithium content. Dielectric constant decreases with the increase of x value when $x > 0.1$ due to the substitution of lower polar Li ion for Nd^{3+} . The dielectric constant of the sample with $x = 0$ is much lower than that of other compositions, which is related to the existence of low k $\text{Nd}_2\text{Ti}_2\text{O}_7$ phase. All samples exhibit negative τ_f value, and its absolute value decreases from 256 to about 20 ppm/°C as the lithium content decreases from $x = 0.5$ to 0.1.

Acknowledgements

This work was supported by the Natural Science Foundation of China (NSFC), (project no.: 50572060), key funding for basic research of Shanghai Science and Technology Committee (06JC14070) and sponsored by Shanghai Pujiang Program(D).

References

- [1] Y. Harada, T. Ishigaki, H. Kawai, J. Kuwano, Lithium ion conductivity of polycrystalline perovskite $\text{La}_{0.67-x}\text{Li}_{3x}\text{TiO}_3$ with ordered and disordered arrangements of the A-site ions, *Solid State Ionics* 108 (1998) 407–413.
- [2] Y. Inaguma, T. Katsumata, M. Itoh, Y. Morii, Crystal structure of a lithium ion-conducting perovskite $\text{La}_{2/3-x}\text{Li}_{3x}\text{TiO}_3$ ($x = 0.05$), *J. Solid State Chem.* 166 (2002) 67–72.
- [3] M.L. Sanjuan, M.A. Laguna, Raman study of antiferroelectric instability in $\text{La}_{2-x/3}\text{Li}_x\text{TiO}_3$ ($0.1 \leq x \leq 0.5$) double perovskites, *Phys. Rev. B* 64 (2001), 174305-1–174305-5.
- [4] M.A. Laguna, M.L. Sanjuan, A. Varez, J. Sanz, Lithium dynamics and disorder effects in the Raman spectrum of $\text{La}_{2-x/3}\text{Li}_x\text{TiO}_3$, *Phys. Rev. B* 66 (2002), 054301-1–054301-7.
- [5] J. Ibrra, A. Varez, J. Santanmaria, L.M. Torres, J. Sanz, Influence of composition on the structure and conductivity of the fast ionic conductors $\text{La}_{2/3-x}\text{Li}_{3x}$ ($0.03 \leq x \leq 0.167$), *J. Solid State Ionics* 134 (2000) 219–228.
- [6] M.A. Paris, J. Sanz, C. Leon, J. Santanmaria, J. Ibrra, A. Varez, Li mobility in the orthorhombic $\text{Li}_{0.18}\text{La}_{0.61}\text{TiO}_3$ perovskite studied by NMR and impedance spectroscopies, *Chem. Mater.* 12 (2000) 1694–1701.
- [7] Y. Inaguma, C. Liquean, M. Itoh, T. Nakamura, High ionic conductivity in lithium lanthanum titanate, *Solid State Commun.* 86 (10) (1993) 689–693.
- [8] A.D. Robertson, S. Garcia Martin, A. Coats, A.R. West, Phase diagram and crystal chemistry in the Li^+ ion conducting perovskites, $\text{Li}_{0.5-x}\text{RE}_{0.5+x}\text{TiO}_3$: RE = La, Nd, *J. Mater. Chem.* 5 (9) (1995) 1405–1412.
- [9] S. Garcia-Martin, F. Garcia-Alvarado, A.D. Robertson, A.R. West, M.A. Alario-Franco, Microstructural study of the Li^+ ion substituted perovskites $\text{Li}_{0.5-3x}\text{Nd}_{0.5+x}\text{TiO}_3$, *J. Solid State Chem.* 128 (1997) 97–101.
- [10] J.M.S. Skakle, G.C. Mather, M. Morales, R.I. Smith, A.R. West, Crystal structure of the Li^+ ion-conducting phases, $\text{Li}_{0.5-3x}\text{RE}_{0.5+x}\text{TiO}_3$: RE = Nd, Pr; $x = 0.05$, *J. Mater. Chem.* 5 (11) (1995) 1807–1808.
- [11] J.J. Bian, K. Yan, G.X. Song, Structure and microwave dielectric properties of $\text{La}_{2-x/3}\text{Na}_x\text{TiO}_3$, *J. Electroceram.* doi:10.1007/s10832-007-9089-3s.
- [12] R.D. Shannon, C.T. Prewitt, Effective ionic radii in oxides and fluorides, *Acta Crystallogr. B* 25 (1969) 925–944.
- [13] I.M. Reaney, E. Colla, N. Setter, Dielectric and structural characteristics of Ba- and Sr-based complex perovskites as a function of tolerance factor, *Jpn. J. Appl. Phys.* 33 (1994) 3984–3990.
- [14] V.J. Fratello, C.D. Brandle, *J. Mater. Res.* 9 (10) (1994) 2554.
- [15] H. Takahashi, K. Kageyama, K. Kodaira, Microwave dielectric properties of lanthanide titanate ceramics, *Jpn. J. Appl. Phys.* 32 (1993) 4327–4331.